Inorg. Chem. **2004**, *43*, 7774–7783

Complexes Having the *fac*-$\{M(CO)_3\}^+$ Core (M = Tc, Re) Useful in Radiopharmaceuticals: X-ray and NMR Structural Characterization and Density Functional Calculations of Species Containing Two sp^3 N Donors and One sp^3 O Donor

Malgorzata Lipowska,[†] Renzo Cini,[‡] Gabriella Tamasi,[‡] Xiaolong Xu,[†] Andrew T. Taylor,[†] and Luigi G. Marzilli[§,*]

Department of Radiology, Emory University, Atlanta, Georgia 30322, Department of Chemistry, Louisiana State University, Baton Rouge, Louisiana 70803, and Department of Chemical and Biosystem Sciences and Technologies, University of Siena, I-53100 Siena, Italy

Received April 6, 2004

Radiopharmaceuticals containing the "*fac*-$\{M(CO)_3\}^+$" core (M = ^{99m}Tc, ^{186}Re, or ^{188}Re) have potential as diagnostic or therapeutic agents. Complexes with this core with sp^3 amine donors have received little attention. We have studied adducts formed by ENDACH$_2$ ($HO_2CCH_2NHCH_2CH_2NHCH_2CO_2H$) and ENACH ($NH_2CH_2CH_2NHCH_2CO_2H$). $Re(CO)_3$(ENDACH)-A (**1A**) and $Re(CO)_3$(ENDACH)-B (**1B**) isomers were obtained by the reaction of ENDACH$_2$ with $Re(CO)_5Cl$. $Re(CO)_3$(ENAC) (**2**) was obtained by the reaction of ENACH with aqueous $[Re(CO)_3(H_2O)_3]^+$. From single-crystal X-ray data, the three new neutral complexes, **1A**, **1B**, and **2**, have a six-coordinate, pseudo-octahedral Re center with facially coordinated carbonyl ligands. ENDACH$^-$ and ENAC$^-$ bind facially to Re through both amine nitrogens and one carboxyl oxygen, forming two five-membered chelate rings. The $Re(CO)_3$(ENDACH) isomers have an uncoordinated, dangling $-CH_2CO_2H$ group, which is an ideal coupling site for attachment to biomolecules. The isomers differ by the configuration of the NH center bearing this dangling group. The H atom of the amine (N2) is endo (near the carbonyl ligands in the basal plane) in **1A** and exo (away from carbonyl ligands) in isomer **1B**. Isomers reach equilibrium (**1A**:**1B**, 70:30) after 3 days at high pH. Density functional structure optimizations were performed for isolated molecules of the type $Tc^I/Re^I(CO)_3(N_2O)$: $[Re(CO)_3(NH_3)_2(H_2O)]^+$, $[Tc(CO)_3(NH_3)_2(H_2O)]^+$, $[Re(CO)_3(EN)(H_2O)]^+$ (EN, ethylenediamine), $[Tc(CO)_3(EN)(H_2O)]^+$, and various models for **1A**, **1B**, and **2**. The computed structures are in good agreement with the X-ray structures. The theoretical and experimental Re–N bond distances usually agree within 0.045 Å. The total electronic energy values for the computed **1A** and **1B** models differ by 0.815 kcal mol^{-1}, giving an isomer ratio of 80:20, in good agreement with the **1A**/**1B** ratio (70:30) found.

Introduction

In our search for superior anionic and cationic ^{99m}Tc renal imaging agents, we are exploring possible radiopharmaceuticals containing the *fac*-$\{^{99m}Tc(CO)_3\}^+$ moiety. A fully aqueous kit preparation of the organometallic complex, $[^{99m}Tc(CO)_3(H_2O)_3]^+$, directly from $^{99m}TcO_4^-$ was recently developed.[1,2] Because the aqua ligands are labile and readily substituted, ligands with desired physiochemical properties and targeting components can be introduced. The Tc core determines the ligand design, namely, the choice of donor atoms, the numbers of donor atoms, and the geometrical arrangement of donors. Previous experiments showed that ligands containing aromatic sp^2 N-heterocycles (e.g., imidazole, pyridine, pyrazole, and pyrazine) readily form complexes in high yield from the *fac*-$[M(CO)_3(H_2O)_3]^+$ precursor (M = Tc, Re).[3−7] A few examples of tricarbonyl complexes with only aliphatic amines as donors have been

* Author to whom correspondence should be addressed. Phone: 225-578-0933. Fax: 225-578-3463. E-mail: lmarzil@lsu.edu.
[†] Emory University.
[‡] University of Siena.
[§] Louisiana State University.

(1) Alberto, R.; Schibli, R.; Egli, A.; Schubiger, A. P. *J. Am. Chem. Soc.* **1998**, *120*, 7987.
(2) Alberto, R.; Ortner, K.; Wheatley, N.; Schibli, R.; Schubiger, A. P. *J. Am. Chem. Soc.* **2001**, *123*, 3135.

10.1021/ic049544i CCC: $27.50
Published on Web 10/23/2004

Chart 1

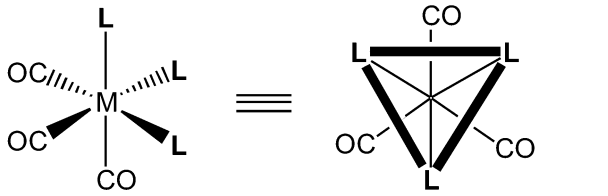

Normal view of octahedral molecule

View of octahedral molecule along three-fold axis

reported.[4,5,8,9] Preferred multidentate ligands for radiopharmaceuticals adopt "geometries" allowing tridentate binding to one face of an octahedron (Chart 1).

In a program directed at identifying a renal agent, we selected the ethylenediamine-*N*,*N*′-diacetic acid ($ENDACH_2$) ligand, which has two secondary amine and two carboxylic acid groups, because we anticipated that a $[^{99m}Tc(CO)_3(ENDAC)]^-$ agent with a free carboxyl group useful for renal targeting of anionic agents would form from $[^{99m}Tc(CO)_3(H_2O)_3]^+$. Two radiochemical products, $^{99m}Tc(CO)_3$(ENDAC)-A (Tc-A) and $^{99m}Tc(CO)_3$(ENDAC)-B (Tc-B) (defined by the order of HPLC elution), formed in a 1:1 ratio at the optimal labeling conditions (PBS buffer pH 7.4) and were separated by HPLC.[10] In our rat model, the Tc-A and Tc-B isomers showed high specificity for renal excretion (56 ± 6% and 90 ± 4% for Tc-A at 10 and 60 min, respectively, and 49 ± 6% and 86 ± 4% for Tc-B at 10 and 60 min, respectively, of that of ^{131}I-ortho-iodohippuran (OIH)). (OIH is the internal standard for measurement of effective renal plasma flow.[11]) The biodistribution data show gut and liver activity comparable to that of OIH.[10] These promising results support further synthesis and testing of the entirely new types of renal agents made available by this core. Therefore, an investigation of the source of the isomer formation and the aqueous chemistry of relevant amine complexes was warranted. Because all isotopes of Tc are radioactive, Re analogues of investigational ^{99m}Tc radiopharmaceuticals are routinely prepared for characterization. Analogous Tc and Re complexes have virtually identical physical properties, allowing correlation of distribution findings obtained by using ^{99m}Tc with the structural properties of the Re derivatives.[12,13] In previous work with more traditional $^{99m}Tc^{V}O$ radiopharmaceuticals, X-ray structural characterization, NMR solution studies, and computer modeling were useful in interpreting the complicated solution behavior arising from the presence of coordinated secondary amines and of dangling carboxyl groups. Thus, we investigated applying this multipronged approach to the *fac*-$M(CO)_3$ complexes.

Experimental Section

$Re(CO)_5Cl$, ethylenediamine-*N*,*N*′-diacetic acid ($ENDACH_2$), and all solvents were purchased from Aldrich and were used without purification. Ethylenediamine-*N*-acetic acid (ENACH) was purchased from Bachem and was used without purification. The precursor, $[Et_4N]_2[Re(CO)_3Br_3]$, was prepared as reported in the literature.[14] Elemental analyses were performed by Atlantic Microlabs, Atlanta, GA. ^{1}H NMR spectra were recorded on Varian INOVA 400- or 600-MHz spectrometers and referenced to internal sodium 3-(trimethylsilyl)propionate-d_4. ^{1}H NMR spectra were simulated by using ACD/HNMR software.[15] ACD/HNMR software allows calculation of exact spectra for any strongly coupled system and uses a structure-fragment approach to predict ^{1}H NMR spectra. The signals were simulated separately for each spin system by using the chemical shifts from the one-dimensional (1D) ^{1}H NMR spectrum. The coupling constants were changed systematically until the best fit between the experimental and calculated multiplet patterns was found. FTIR spectra were recorded (KBr pellets) on a Nicolet 510 FT IR instrument. HPLC analyses were performed on a Waters Breeze system equipped with Waters 2487 dual wavelength absorbance detector, Waters 1525 binary pump, and XTerra MS C18 column (5 μm; 4.6 × 250 mm). High-performance liquid chromatography (HPLC) solvents consisted of aqueous pH 2.5 0.05 M TEAP (triethylammonium phosphate, solvent A) and methanol (solvent B) with the gradient method.[4]

Syntheses of $Re(CO)_3$(ENDACH). Method A. $Re(CO)_5Cl$ (0.3 g, 0.83 mmol) and $ENDACH_2$ (0.146 g, 0.83 mmol) were dissolved in MeOH/H_2O (1:1, 20 mL), the pH of the reaction mixture was adjusted to pH 7 with 1 N NaOH, the solution was refluxed, and the progress of the reaction was monitored by HPLC. Two products formed in an ~2:1 ratio, which did not change after 4 h of heating. The solution was allowed to cool to room temperature, and the pH was adjusted to pH 2 with 1 N HCl. The volume was reduced by rotary evaporation to ~5 mL, and the solution was left overnight at 4 °C. A white solid (0.21 g, 57%) was collected, washed with cold water, and vacuum-dried. The ^{1}H NMR spectrum (D_2O) indicated that the product was an ~2:1 mixture of two isomers ($Re(CO)_3$(ENDACH)-A (**1A**) and $Re(CO)_3$(ENDACH)-B (**1B**)), which were separated by slow, fractional crystallization from water as flat, square, colorless crystals of **1A** and colorless prisms of **1B**. Both products are slightly soluble in water.

Method B. $Re(CO)_5Cl$ (0.3 g, 0.83 mmol) and $ENDACH_2$ (0.146 g, 0.83 mmol) were suspended in THF/H_2O (1:1, 20 mL), and without adjusting the pH from 4, the reaction mixture was maintained at reflux for 3 h. Upon being heated, the mixture became

(3) Alberto, R.; Schibli, R.; Waibel, R.; Abram, U.; Schubiger, A. P. *Coord. Chem. Rev.* **1999**, *190*−*192*, 901.
(4) Schibli, R.; La Bella, R.; Alberto, R.; Garcia-Garayoa, E.; Ortner, K.; Abram, U.; Schubiger, P. A. *Bioconjugate Chem.* **2000**, *11*, 345.
(5) Schibli, R.; Schwarzbach, R.; Alberto, R.; Ortner, K.; Schmalle, H.; Dumas, C.; Egli, A.; Schubiger, P. A. *Bioconjugate Chem.* **2002**, *13*, 750.
(6) Banerjee, S. R.; Levadala, M. K.; Lazarova, N.; Wei, L.; Valliant, J. F.; Stephenson, K. A.; Babich, J. W.; Maresca, K. P.; Zubieta, J. *Inorg. Chem.* **2002**, *41*, 6417.
(7) Grundler, P. V.; Salignac, B.; Cayemittes, S.; Alberto, R.; Merbach, A. E. *Inorg. Chem.* **2004**, *43*, 865.
(8) Egli, A.; Alberto, R.; Tannahill, L.; Schibli, R.; Abram, U.; Schaffland, A.; Waibel, R.; Tourwe, D.; Jeannin, L.; Iterbeke, K.; Schubiger, P. A. *J. Nucl. Med.* **1999**, *40*, 1913.
(9) Mundwiler, S.; Candreia, L.; Hafliger, P.; Ortner, K.; Alberto, R. *Bioconjugate Chem.* **2004**, *15*, 195.
(10) Lipowska, M.; Hansen, L.; Marzilli, L. G.; Taylor, A. *J. Nucl. Med.* **2001**, *424*, 259P.
(11) Fritzberg, A. R. *J. Nucl. Med. Technol.* **1984**, *12*, 177.
(12) Pietzsch, H.-J.; Gupta, A.; Reisgys, M.; Drews, A.; Seifert, S.; Syhre, R.; Spies, H.; Alberto, R.; Abram, U.; Schubiger, P. A.; Johannsen, B. *Bioconjugate Chem.* **2000**, *11*, 414.
(13) Kramer, D.; Mahmood, A.; Davison, A.; Jones, A. G. In *Abstract of Papers, 225th ACS National Meeting*; American Chemical Society: New Orleans, LA, 2003.
(14) Alberto, R.; Egli, A.; Abram, U.; Hegetschweiler, K.; Gramlich, V.; Schubiger, P. A. *J. Chem. Soc., Dalton Trans.* **1994**, 2815.
(15) *ACD/HNMR*, version 1.0; Advanced Chemistry Development, Inc.: Toronto, ON, Canada, 1996 (http://www.acdlabs.com).

a clear solution, which was cooled to room temperature and taken to dryness. Water (5 mL) was added to the residue, which dissolved upon heating at 50 °C for a few minutes. A white solid, which precipitated after the solution was left overnight at 5 °C, was collected by filtration, washed with a small amount of cold water, and dried in vacuo. Yield, 0.1 g (27%) of pure isomer **1B**.

Method C. $ENDACH_2$ (12 mg, 0.065 mmol) and $[Et_4N]_2[Re(CO)_3Br_3]$ (50 mg, 0.065 mmol) were suspended in H_2O (2 mL). The pH of the mixture was adjusted to pH ≈ 7 with 2 N NaOH, and the clear solution was stirred at room temperature for 16 h. The pH was adjusted to pH 2 with 1 N HCl, and HPLC analysis of the reaction mixture revealed the presence of only one major product. The solution was concentrated by rotary evaporation to ∼1 mL and stored at 5 °C overnight. A white precipitate was collected, washed with a small amount of cold water, and vacuum-dried. Yield, 15 mg (51%) of pure isomer **1B**.

$Re(CO)_3$(ENDACH)-A·H_2O (1A). Anal. Calcd for $C_9H_{11}N_2O_7Re·H_2O$: C, 23.32; H, 2.83; N, 6.05. Found: C, 23.37; H, 2.86; N, 6.04. ^{1}H NMR (D_2O, pH 3.2): 2.34 (m, 1H), 3.14 (m, 3H), 3.51 (dd, J = 16.8, 5.4 Hz, 1H), 3.54 (d, J = 18 Hz, 1H), 3.75 (dd, J = 16.8, 6.6 Hz, 1H), 3.91 (dd, J = 17.4, 7.2 Hz, 1H), 5.45 (bs, 1H), 6.43 (bs, 1H). IR (KBr, cm^{-1}): 3193 (m), 2948 (w), 2021 (s), 1923 (s), 1901 (s), 1732 (m), 1634 (s), 1398 (m), 1057 (w), 922 (w).

$Re(CO)_3$(ENDACH)-B (1B). Anal. Calcd for $C_9H_{11}N_2O_7Re$: C, 24.27; H, 2.49; N, 6.29. Found: C, 24.06; H, 2.51; N, 6.38. ^{1}H NMR (D_2O, pH 3.1): 2.82 (m, 2H), 2.98 (m, 1H), 3.31 (m, 1H), 3.59 (d, J = 17.2 Hz, 1H), 3.86 (dd, J = 16.8, 7.6 Hz, 1H), 3.92 (dd, J = 17.2, 6.4 Hz, 1H), 4.02 (dd, J = 17.2, 6.0 Hz, 1H), 5.03 (bs, 1H), 6.44 (bs, 1H). IR (KBr, cm^{-1}): 3272 (m), 3125 (m), 2916 (w), 2021 (s), 1900 (s), 1883 (s), 1722 (m), 1645 (m), 1576 (m), 1212 (w), 1047 (w), 970 (w).

Synthesis of $Re(CO)_3$(ENAC) (2). ENACH (0.05 g, 0.423 mmol), dissolved in 2 mL of water, was treated with 4.23 mL of a 0.1 M solution of $[Re(CO)_3(H_2O)_3][OTf]$.[16] The pH of the mixture was adjusted to pH ≈ 7 with 2 N NaOH, and the solution was refluxed for 1 h. Analysis of the reaction mixture by HPLC revealed the presence of only one major product. The solution was allowed to cool to room temperature and taken to dryness. The white solid was washed with a small amount of cold water and ethanol, vacuum-dried, and recrystallized from water/ethanol (1:1). Yield, 0.11 g (67%). Anal. Calcd for $C_7H_9N_2O_5Re$: C, 21.70; H, 2.34; N, 7.23. Found: C, 21.78; H, 2.35; N, 7.21. ^{1}H NMR (D_2O): 2.56 (m, 1H), 3.00 (m, 3H), 3.51 (d, J = 17.4 Hz, 1H), 3.82 (d, J = 17.4 Hz, 1H), 4.24 (bs, 1H). ^{1}H NMR (DMSO): 2.40 (m, 1H), 2.69 (m, 1H), 2.79 (m, 1H), 2.89 (m, 1H), 3.31 (d, J = 16.8 Hz, 1H), 3.48 (dd, J = 16.8, 7.2 Hz, 1H), 4.92 (m, 1H), 4.98 (m, 1H), 6.87 (m, 1H).

X-ray Crystal Structural Determination. Suitable crystals of **1A**, **1B**, and **2** were coated with Paratone N oil, suspended in a small fiber loop, and placed in a cooled nitrogen gas stream at 100 K on a Bruker D8 SMART APEX CCD sealed tube diffractometer with graphite monochromated Mo Kα (0.71073 Å) radiation (for **1A** and **1B**) and Cu Kα (1.54178 Å) radiation (for **2**). A hemisphere of data was measured by using a series of combinations of φ and ω scans with 10-s frame exposures and 0.3° frame widths. Data collection, indexing, and initial cell refinements were carried out with SMART[17] software. SAINT[18] software was used for frame integration and final cell refinements. Final cell parameters were determined from least-squares refinement on 8389 reflections. The SADABS[19] program was used to carry out absorption corrections.

The structures were solved by using direct methods and difference Fourier techniques (SHELXTL, v5.10).[20] All atoms (including hydrogen) were located in difference Fourier maps; all non-hydrogen atoms were refined anisotropically, and hydrogen atoms were refined isotropically in the final cycles of least squares. Scattering factors and anomalous dispersion corrections were taken from the *International Tables for X-ray Crystallography*.[21] Structure solution, refinement, graphics, and generation of publication materials were performed by using SHELXTL, v5.10 software. Crystal data and refinement parameters for **1A**, **1B**, and **2** are listed in Table 1. Selected bond distances and angles appear in Table 2 and Table 3, respectively.

Density Functional Calculations. All density functional calculations were performed by using the GAUSSIAN98, revision A.7[22] package implemented on an Origin 3800 SG machine at CINECA (Inter-University Computing Center, Casalecchio di Reno, Bologna, Italy). Geometry optimizations, population analysis, and vibrational frequency calculations were obtained by using the Becke3LYP[23] method and the LANL2DZ[23] basis set. Models analyzed include the following (ethylenediamine ring pucker indicated by δ-EN or

Table 1. Crystal Data and Structure Refinement for $Re(CO)_3$(ENDACH)-A·H_2O (**1A**), $Re(CO)_3$(ENDACH)-B (**1B**), and $Re(CO)_3$(ENAC)·H_2O (**2**)

	1A	1B	2
empirical formula	$C_9H_{13}N_2O_8Re$	$C_9H_{11}N_2O_7Re$	$C_7H_{11}N_2O_6Re$
fw	463.41	445.40	405.38
T (K)	100 (2)	100 (2)	100 (2)
λ (Å)	0.71073	0.71073	1.54178
crystal system	orthorhombic	monoclinic	monoclinic
space group	$P2_12_12_1$	$P2_1/c$	$P2_1/n$
unit cell dimensions			
a (Å)	7.457 (9)	8.426 (9)	7.077 (2)
b (Å)	10.751 (12)	10.763 (11)	19.091 (1)
c (Å)	16.739 (19)	13.096 (14)	8.238 (1)
β (deg)		98.10 (1)	90.61 (1)
V (Å^3)	1341.9 (3)	1175.9 (2)	1112.9 (1)
Z	4	4	4
ρ_{calc}(mg/m^3)	2.294	2.516	2.419
abs coeff (mm^{-1})	9.094	10.367	21.567
R indices [$I > 4\sigma(I)$]	$R_1 = 0.0211$[a]	$R_1 = 0.0262$	$R_1 = 0.0309$
	$wR_2 = 0.0509$[b]	$wR_2 = 0.0654$	$wR_2 = 0.0821$
R indices (all data)	$R_1 = 0.0216$	$R_1 = 0.0283$	$R_1 = 0.0336$
	$wR_2 = 0.0510$	$wR_2 = 0.0664$	$wR_2 = 0.0837$

[a] $R_1 = (\sum||F_o| - |F_c||)/\sum|F_o|$. [b] $wR_2 = [\sum[w(F_o^2 - F_c^2)^2]/\sum[w(F_o^2)^2]]^{1/2}$ where $w = 1/[\sigma^2(F_o^2) + (aP)^2 + bP]$ and $P = [(\text{Max};0, F_o^2) + 2F_c^2]/3$.

(16) He, H.; Lipowska, M., Unpublished data.
(17) *SMART*, version 5.55; Bruker AXS, Inc.: Madison, WI, 2000.
(18) *SAINT*, version 6.02; Bruker AXS, Inc.: Madison, WI, 1999.
(19) Sheldrick, G. *SADABS*: University of Gottingen, Gottingen, Germany, 1996.
(20) *SHELXTL*, version 5.10; Bruker AXS, Inc.: Madison, WI, 1997.
(21) *International Tables for X-ray Crystallography*; Wilson, A. J. C.; Ed.; Vol. C; Kluwer Academic Publishers: Dordrecht, The Netherlands; 1992; pp 500−502 and pp 219−222 (Tables 6.1.1.4 and 4.2.6.8).
(22) Frisch, M. J.; Trucks, G. W.; Schlegel, H. B.; Scuseria, G. E.; Robb, M. A.; Cheeseman, J. R.; Zakrzewski, V. G.; Montgomery, J. A., Jr.; Stratmann, R. E.; Burant, J. C.; Dapprich, S.; Millam, J. M.; Daniels, A. D.; Kudin, K. N.; Strain, M. C.; Farkas, O.; Tomasi, J.; Barone, V.; Cossi, M.; Cammi, R.; Mennucci, B.; Pomelli, C.; Adamo, C.; Clifford, S.; Ochterski, J.; Petersson, G. A.; Ayala, P. Y.; Cui, Q.; Morokuma, K.; Malick, D. K.; Rabuck, A. D.; Raghavachari, K.; Foresman, J. B.; Cioslowski, J.; Ortiz, J. V.; Stefanov, B. B.; Liu, G.; Liashenko, A.; Piskorz, P.; Komaromi, I.; Gomperts, R.; Martin, R. L.; Fox, D. J.; Keith, T.; Al-Laham, M. A.; Peng, C. Y.; Nanayakkara, A.; Gonzalez, C.; Challacombe, M.; Gill, P. M. W.; Johnson, B. G.; Chen, W.; Wong, M. W.; Andres, J. L.; Head-Gordon, M.; Replogle, E. S.; Pople, J. A. *Gaussian 98*, revision A.7; Gaussian, Inc.: Pittsburgh, PA, 1998.
(23) Frish, A.; Frisch, M. J. *Gaussian 98 User's Reference*, 2nd ed.; Gaussian, Inc.: Pittsburgh, PA, 1998.

Table 2. Selected Bond Distances (Å) for X-ray Structures **1A**, **1B**, and **2**; and for Computed Molecules **3**, **4**, **5**, **6**, **7a**, **7b**, **8a**, **8b**, **9a**, **9b**, and **9c** (cf. Figures for Atom Labeling)

	distance													
vector	**1A**	**1B**	**2**	**3**[a]	**4**[b]	**5**	**6**	**7a**	**7b**	**8a**	**8b**	**9a**	**9b**	**9c**
M1−O1	2.150	2.145	2.149	2.276	2.286	2.284	2.293	2.139	2.130	2.146	2.136	2.153	2.144	2.144
M1−N1	2.208	2.211	2.210	2.267	2.275	2.259	2.264	2.257	2.246	2.259	2.246	2.252	2.253	2.249
M1−N2	2.248	2.259	2.218	2.266	2.274	2.240	2.245	2.226	2.249	2.229	2.253	2.216	2.230	2.231
M1−C7	1.902	1.905	1.908	1.905	1.910	1.902	1.906	1.911	1.912	1.916	1.917	1.907	1.909	1.907
M1−C8	1.924	1.920	1.929	1.926	1.934	1.928	1.936	1.921	1.922	1.927	1.928	1.921	1.918	1.921
M1−C9	1.913	1.913	1.914	1.926	1.934	1.931	1.939	1.921	1.919	1.927	1.924	1.921	1.919	1.919
O1−C1	1.287	1.280	1.284					1.338	1.333	1.335	1.331	1.326	1.323	1.324
O2−C1	1.240	1.250	1.248					1.247	1.249	1.249	1.251	1.254	1.255	1.254
O3−C6	1.217	1.206										1.304	1.304	1.276
O4−C6	1.329	1.313										1.272	1.272	1.297
O5−C7	1.163	1.152	1.155	1.183	1.179	1.184	1.181	1.195	1.195	1.190	1.190	1.198	1.197	1.197
O6−C8	1.160	1.152	1.141	1.182	1.178	1.182	1.178	1.186	1.186	1.183	1.182	1.188	1.189	1.188
O7−C9	1.159	1.150	1.166	1.182	1.178	1.182	1.178	1.188	1.188	1.184	1.184	1.194	1.195	1.195
O1−H1O				0.978	0.978	0.978	0.977							
N1−C2	1.491	1.484	1.473					1.513	1.511	1.510	1.508	1.507	1.507	1.507
N1−C3	1.486	1.494	1.494			1.515	1.511	1.517	1.508	1.514	1.507	1.517	1.512	1.512
N2−C4	1.491	1.501	1.500			1.515	1.511	1.503	1.510	1.500	1.506	1.505	1.505	1.509
N2−C5	1.477	1.483										1.514	1.514	1.513
N1−H1N	0.823	0.990	0.930	1.025	1.024	1.025	1.025	1.023	1.022	1.022	1.022	1.022	1.022	1.022
N2−H2NA	0.727	0.975	0.920	1.025	1.024	1.025	1.025	1.028	1.025	1.028	1.022	1.051	1.048	1.041
N2−H2NB			0.920			1.025	1.025	1.022	1.022	1.021	1.024			
C1−C2	1.521	1.510	1.516					1.554	1.552	1.555	1.553	1.556	1.553	1.554
C5−C6	1.520	1.511										1.575	1.576	1.573
C3−C4	1.512	1.518	1.517			1.530	1.531	1.534		1.534		1.527	1.528	1.529

[a] The O−H bond distances for **3** were restrained to refine to the same value. [b] The N−H bond distances for **4** were restrained to refine to the same value.

Table 3. Selected Angles (deg) for X-ray Structures **1A**, **1B**, and **2** and for Computed Molecules **3**, **4**, **5**, **6**, **7a, 7b**, **8a**, **8b**, **9a**, **9b**, and **9c** (cf. Figures for Atom Labeling)

	angle													
vectors	**1A**	**1B**	**2**	**3**	**4**	**5**	**6**	**7a**	**7b**	**8a**	**8b**	**9a**	**9b**	**9c**
N1−M1−O1	76.2	76.6	76.5	83.2	84.0	84.6	85.5	73.9	76.4	74.4	77.1	74.0	76.1	76.0
N2−M1−O1	82.5	80.2	80.9	82.7	83.9	83.0	83.9	78.7	76.9	79.5	77.6	86.0	82.7	81.2
N2−M1−N1	78.5	78.9	78.1	84.5	85.4	78.0	78.4	78.1	78.9	78.5	79.4	79.2	79.2	79.7
C7−M1−O1	174.1	173.5	172.7	175.7	176.2	176.6	177.0	170.6	170.6	171.5	171.6	172.7	172.5	172.6
C8−M1−O1	98.9	95.0	96.6	93.0	92.9	92.2	91.9	96.6	95.5	95.8	94.7	96.8	96.0	96.1
C9−M1−O1	94.0	97.8	96.0	93.3	93.0	92.9	92.8	96.0	96.8	95.3	96.0	91.9	93.5	93.3
C7−M1−N1	98.1	99.3	97.8	93.8	93.3	92.9	92.6	98.7	96.9	98.9	96.9	98.9	97.4	97.1
C7−M1−N2	94.9	94.1	93.5	94.0	93.2	94.2	93.5	94.3	95.5	94.2	95.6	90.8	92.5	94.8
C8−M1−N1	173.2	171.1	172.4	175.6	176.4	173.5	173.7	169.5	170.8	169.1	170.8	169.4	171.1	170.6
C8−M1−N2	96.3	96.8	97.7	92.8	92.4	96.1	95.7	95.8	95.1	95.4	94.8	95.1	95.9	94.3
C9−M1−N1	97.0	96.9	96.1	92.6	92.2	95.7	95.7	95.7	95.4	95.7	95.1	95.3	94.4	95.1
C9−M1−N2	174.8	175.7	173.9	175.3	176.3	172.7	173.4	172.7	172.3	173.0	172.3	174.5	173.2	173.2
C7−M1−C8	86.6	88.8	88.7	89.8	89.7	90.0	89.8	90.3	90.6	90.5	90.7	90.0	90.2	90.5
C7−M1−C9	88.2	87.7	89.1	89.9	89.8	89.7	89.7	90.4	90.3	90.5	90.5	90.7	90.6	90.2
C9−M1−C8	87.9	87.1	87.9	89.9	89.7	90.1	90.1	89.7	89.9	89.7	89.9	90.2	90.2	90.3
M1−O1−C1	117.3	118.0	118.4					119.4	120.6	118.7	119.7	119.3	120.2	120.1
M1−N1−C2	109.0	108.9	109.1					105.7	108.3	105.2	107.7	106.9	108.2	108.2
M1−N1−C3	109.6	108.8	109.1			110.6	109.7	111.1	108.2	110.4	107.6	109.9	108.4	108.2
M1−N2−C4	109.0	108.6	111.3			109.8	109.3	108.6	111.1	108.1	110.4	107.6	109.5	109.2
M1−N2−C5	116.0	116.9										120.5	121.3	118.7
M1−C7−O5	178.4	178.7	178.7	180.0	180.0	180.0	180.0	180.0	180.0	180.0	180.0	180.0	180.0	180.0
M1−C8−O6	178.2	177.0	177.9	180.0	180.0	180.0	180.0	180.0	180.0	180.0	180.0	180.0	180.0	180.0
M1−C9−O7	178.7	177.4	178.4	180.0	180.0	180.0	180.0	180.0	180.0	180.0	180.0	180.0	180.0	180.0
C3−N1−C2	113.8	111.6	112.2					110.9	114.0	111.2	114.2	111.2	113.7	113.8
C5−N2−C4	112.6	109.1										111.2	109.6	110.4
N1−C2−C1	111.7	110.7	112.0					108.4	111.3	108.9	111.8	109.2	112.0	112.0
N1−C3−C4	109.7	109.1	109.2			109.0	109.3	111.6	110.4	111.8	110.7	110.4	109.9	110.0
N2−C4−C3	108.6	109.1	107.5			108.5	108.9	108.6	110.1	108.8	110.3	109.2	108.9	109.6
N2−C5−C6	114.0	111.3										107.3	107.8	109.1
O4−C6−O3	120.7	125.1										129.9	129.8	130.4
O1−C1−O2	123.3	123.0	122.9					126.4	126.3	126.4	126.3	126.9	126.8	126.9
O1−C1−C2	117.4	117.1	116.5					113.2	113.8	113.7	114.3	113.9	114.4	114.3
C2−C1−O2	119.2	119.9	120.6					120.4	119.9	120.0	119.4	119.2	118.8	118.8
C5−C6−O3	123.6	111.9										113.3	113.3	116.1
C5−C6−O4	115.8	123.1										116.8	116.8	113.5

λ-EN): $[Re(CO)_3(NH_3)_2(H_2O)]^+$, **3**; $[Tc(CO)_3(NH_3)_2(H_2O)]^+$, **4**; $[Re(CO)_3(EN)(H_2O)]^+$ (EN, ethylenediamine), **5**; $[Tc(CO)_3(EN)(H_2O)]^+$, **6**; $Re(CO)_3$(ENAC), **7a**, δ-EN; $Re(CO)_3$(ENAC), **7b**, λ-EN; $Tc(CO)_3$(ENAC), **8a**, δ-EN; $Tc(CO)_3$(ENAC), **8b**, λ-EN; $[Re(CO)_3(ENDAC)]^-$, isomer A δ-EN −*anticlinal*-CH_2COO^-, **9a**; $[Re(CO)_3(ENDAC)]^-$, isomer A λ-EN −*antiperiplanar*-

CH_2COO^-, **9b**; and $[Re(CO)_3(ENDAC)]^-$, isomer B λ-EN +*antiperiplanar*-CH_2COO^-, **9c**. All models were in the singlet state, in the gas phase, and with the metal configuration shown in the ORTEP drawings below. Geometrical parameters have been fully optimized without symmetry constraints, except that all the C−H bond distances within each molecule were restrained to refine to the same value. The M−C−O bond angles were fixed at 180° for the optimizations. Optimization of the geometry was carried out according to the criteria implemented in GAUSSIAN98 (for maximum force and root mean square (rms) force shifts, 0.000450, 0.000300 hartrees/b, respectively, and for maximum displacement and rms displacement 0.001800, 0.001200 Å, respectively). For some of the species containing the H_2O ligand, the displacements did not meet the GAUSSIAN98 criteria (owing chiefly to the movements of the aqua-hydrogen atoms) but were close to the threshold values; also, the forces were small. For a detailed description of the starting structure used for each molecule see Results and Discussion. Molecular drawings for the optimized models were obtained through the XPMA-ZORTEP[24] and ORTEP32[25] packages.

Results and Discussion

Synthesis. The new complexes, $Re(CO)_3$(ENDACH)-A (**1A**) and $Re(CO)_3$(ENDACH)-B (**1B)**, were synthesized by the stoichiometric reaction of the $ENDACH_2$ ligand with $Re(CO)_5Cl$ or $[Et_4N]_2[Re(CO)_3Br_3]$ under aqueous conditions. The reactions produced different results depending upon the pH and the temperature of the reaction mixture. The progress of the reaction and product formation were monitored by reverse-phase HPLC. In the first reaction (method A) of $ENDACH_2$ with $Re(CO)_5Cl$ at pH 7 and after being heated for 4 h, two isomers **1A** and **1B** were formed in an approximately 2:1 ratio, as confirmed by HPLC (retention time (RT): **1A**, 9 min; **1B**, 11 min) and NMR studies; these isomers were separated by slow, fractional crystallization from water. Only one isomer, $Re(CO)_3$(ENDACH)-B (**1B**), was isolated in 27% yield in a second reaction (method B) when $Re(CO)_5Cl$ was treated with $ENDACH_2$ at pH 4. However, HPLC analysis of the filtrate showed an ∼2:1 ratio for **1A**:**1B**, indicating that isomer **1B** is the major product of the reaction at lower pH and precipitates first. In both methods, a mixture of water and an organic solvent (method A, MeOH; method B, THF) had to be employed because $Re(CO)_5Cl$ is not readily soluble in water. A third method (C) employs the precursor, $[Et_4N]_2[Re(CO)_3Br_3]$, which has the advantage of being soluble in both organic solvents and water. Simple dissolution of $[Et_4N]_2[Re(CO)_3Br_3]$ in water[14] gives $[Re(CO)_3(H_2O)_3]^+$ in the desired *fac*-$Re(CO)_3$ configuration, thus eliminating the need for the harsh reaction conditions required for displacing CO from $Re(CO)_5Cl$. The reaction of the resulting $[Re(CO)_3(H_2O)_3]^+$ cation with the $ENDACH_2$ ligand at room temperature and pH 7 (method C) was closely monitored by HPLC. At 2, 5, and 16 h, the only major product (RT = 11 min) was isomer **1B**. Because of the striking differences in isomer preference depending on the starting Re precursor and the reaction temperature, we performed several experiments by using $[Re(CO)_3(H_2O)_3]^+$ as a precursor and adjusting the reaction temperature. At 50−60 °C, again only one major product (isomer **1B**) formed, but the reaction was complete in the much shorter time of 2 h. When $[Re(CO)_3(H_2O)_3]^+$ and $ENDACH_2$ were refluxed, both isomers formed in an ∼2:1 ratio (**1A**:**1B**), as observed in method A, after just 1 h of heating.

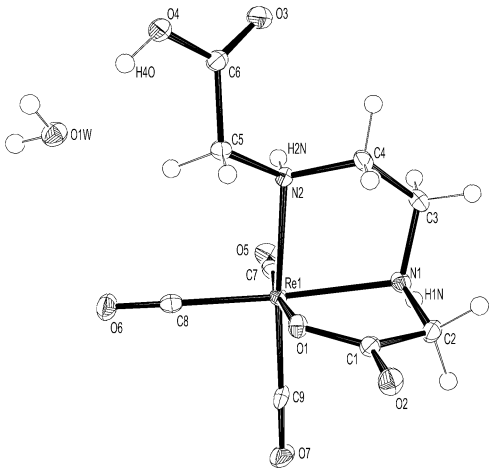

Figure 1. Perspective drawing of $Re(CO)_3$(ENDACH)-A·H_2O (**1A**·H_2O) with 50% probability for the thermal ellipsoids.

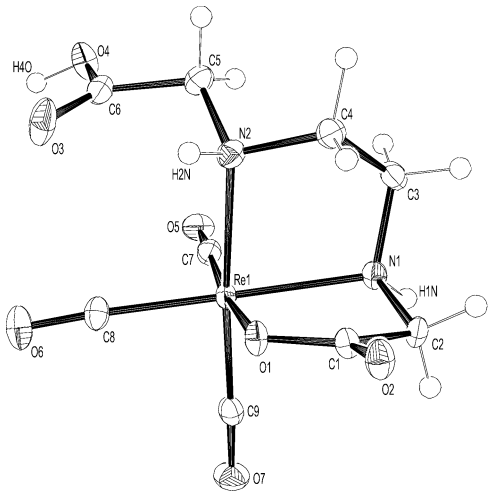

Figure 2. Perspective drawing of $Re(CO)_3$(ENDACH)-B (**1B**) with 50% probability for the thermal ellipsoids.

$Re(CO)_3$(ENAC) (**2**) was obtained (67% yield) by the stoichiometric reaction of ENACH with $[Re(CO)_3(H_2O)_3][OTf]$ under aqueous conditions. Compound **2** was confirmed to be only one species by HPLC (RT = 8.5 min).

X-ray Crystallography. The pseudo-octahedral complexes **1A**, **1B**, and **2** are chiral, neutral monomers with facially coordinated carbonyl ligands. (Re−C bond distances are ∼1.91 Å, with an average C−Re−C bond angle of 87°.) The tridentate $ENDACH_2$ and ENACH ligands coordinate facially through two neutral amines and one carboxyl oxygen, forming two five-membered chelate rings. Each crystal contains one enantiomer in the case of complex **1A**; complexes **1B** and **2** crystallized as racemic mixtures. ORTEP-style drawings in Figures 1, 2, and 3 depict **1A**, **1B**, and **2**, respectively, with the same chirality. This chirality is

(24) Zsolnai, L. *XPMA-ZORTEP 98*; University of Heidelberg, Heidelberg, 1998.

(25) Johnson, C. K.; Burnett, M. N. *ORTEP-3 for Windows*; Oak Ridge National Laboratory: Oak Ridge, TN, 1998 (32-bit implementation by L. J. Farrugia, University of Glasgow).

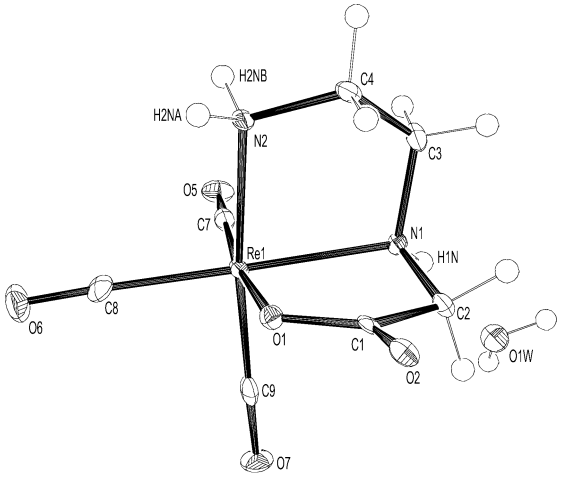

Figure 3. Perspective drawing of $Re(CO)_3(ENAC)\cdot H_2O$ (**2**·H_2O) with 50% probability for the thermal ellipsoids.

maintained throughout this work because the computed models have an EN chelate ring with λ or δ puckers. More importantly, for this chirality, the neutral amine donor anchoring the two chelate rings has the same configuration in all three compounds, with N1 forming a bond to a carbon in each of the chelate rings, a bond to Re and a bond to H1N (Figures 1−3). The Re−N bond distances vary. The Re−N1 distance (2.208(3) Å in **1A** and 2.211(2) Å in **1B**) is shorter than the Re−N2 distance (2.248(3) Å for **1A** and 2.259(2) Å for **1B**), but both complexes have similar values. The Re−N1 distance in **2** is 2.210(4) Å. The Re−N2 distance of 2.218(4) Å in **2** is shorter than that in **1A** and **1B**, as expected because this donor is a primary amine in **2** but a secondary amine in **1A** and **1B**.

The X-ray data establish that **1A** and **1B** are diastereomers. For the same chirality about the metal center, the NH center (N2) bearing the dangling CH_2CO_2H group has a different configuration for the two isomers. The H2N atom of the amine (N2) is endo (near the carbonyl ligands in the basal plane) in **1A** and exo (away from carbonyl ligands) in isomer **1B** (see Chart 2 for numbering of protons). Although under mild conditions isomer **1B** forms preferentially and thus is kinetically preferred, isomer **1A** dominates in the equilibrium mixture (**1A**/**1B**, 70:30), indicating that the endo configuration of the N2 amine, in which the dangling CH_2CO_2H amine substituent extends away from the metal coordination sphere, is favored. Because the dangling carboxyl group in **1A** and **1B** is uncoordinated, it offers an ideal site for functionalization or coupling with a biomolecule.

The other carboxylate groups in **1A** and **1B** are coordinated. The Re−O1 distances, 2.150(2) Å in **1A** and 2.145(18) Å in **1B**, are similar to Re−O1 distances in related compounds in which the ligating oxygen is from a carboxyl group and is coordinated in a position trans to a carbonyl ligand, 2.147(4) Å in $Re(CO)_3$(histidine)[4] and 2.149 Å in $Re(CO)_3$(1-carboxylato-6-carboxy-2,5-dithiohexane).[12] The Re−O1 distance of 2.149(3) Å in **2** is almost identical to those in **1A** and **1B** and is in good agreement with the Re−O bond distance (2.139 Å) computed in the model for **2** (see below).

Chart 2

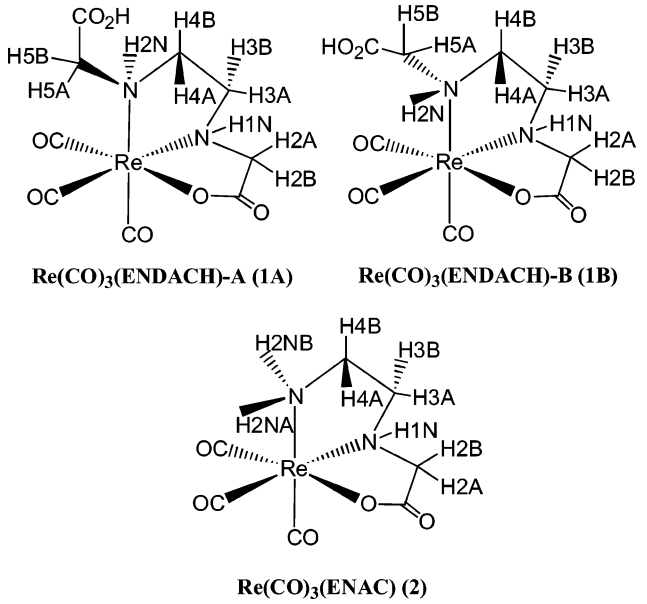

$Re(CO)_3$(ENDACH)-A (1A) **$Re(CO)_3$(ENDACH)-B (1B)**

$Re(CO)_3$(ENAC) (2)

NMR Spectroscopy. An extensive background now exists in interpreting the interrelationship of NMR spectral data such as chemical shifts to dynamic, structural, and protonation states of Re^V oxo compounds that serve as models for radiopharmaceuticals with the M^VO core (M = ^{99m}Tc, ^{186}Re, or ^{188}Re).[26−31] Because we have a closely related group of structurally characterized $Re^I(CO)_3$ adducts, we wanted to take our first steps in developing NMR information as a valuable approach to investigating these types of compounds. One-dimensional ^{1}H NMR spectra of **1A**, **1B**, and **2** were obtained in D_2O at low and high pH, and in DMSO-d_6 (Table 4). Two-dimensional spectra in DMSO-d_6 allowed signal assignments in aqueous solution to be obtained by following the signals in a DMSO-d_6/D_2O mixture. The numbering for the H signals corresponds to the number of the C to which they are bound; C numbering corresponds to that in the X-ray structure; the H atom labels are presented graphically in Chart 2.

The ^{1}H NMR spectrum of $Re(CO)_3$(ENAC) (**2**) in aqueous solution (without adjusting, the solution was pH 7.6) consists of signals from two isolated spin systems, the acetate moiety (coordinated carboxylate; two strongly coupled doublets) and the ethylene bridge (four multiplets in the pattern of one multiplet at 2.56 ppm (integrated for one proton) and three multiplets together at ∼3 ppm (integrated for three protons) (Table 4)). There was also only one very weak, broad signal at 4.24 ppm that could be assigned to an amine group. This signal was not present in the spectrum in D_2O if the pH of

(26) Marzilli, L. G.; Banaszczyk, M. G.; Hansen, L.; Kuklenyik, Z.; Cini, R.; Taylor, A., Jr. *Inorg. Chem.* **1994**, *33*, 4850.
(27) Hansen, L.; Yue, K. T.; Xu, X.; Lipowska, M.; Taylor, A., Jr.; Marzilli, L. G. *J. Am. Chem. Soc.* **1997**, *38*, 88965.
(28) Hansen, L.; Marzilli, L. G.; Taylor, A. Q. *J. Nucl. Med.* **1998**, *42*, 280.
(29) Hansen, L.; Lipowska, M.; Melendez, E.; Xu, X.; Hirota, S.; Taylor, A.; Marzilli, L. G. *Inorg. Chem.* **1999**, *38*, 5351.
(30) Hansen, L.; Hirota, S.; Xu, X.; Taylor, A.; Marzilli, L. G. *Inorg. Chem.* **2000**, *39*, 5731.
(31) Lipowska, M.; Hansen, L.; Cini, R.; Xu, X.; Choi, H.; Taylor, A. T.; Marzilli, L. G. *Inorg. Chim. Acta* **2002**, *339*, 327.

Table 4. ^{1}H NMR (D_2O, DMSO) Chemical Shifts (ppm) and Assignments for $Re(CO)_3$(ENDACH)-A·H_2O (**1A**), $Re(CO)_3$(ENDACH)-B (**1B**), and $Re(CO)_3$(ENAC)·H_2O (**2**)

	C2		C3		C4		C5			
pH	H2A	H2B	H3A	H3B	H4A	H4B	H5A	H5B	H1N	H2N
					1A					
3.2	3.54	3.91	3.13[a]	3.13[a]	2.34	3.13[a]	3.51	3.75	6.43	5.45
12	3.54	3.90	3.13[a]	3.13[a]	2.32	3.13[a]	3.35	3.62		
(DMSO)	3.28	3.42	2.90[a]	2.90[a]	2.15	2.90[a]	3.54	3.64	6.75	5.84
					1B					
3.1	3.59	3.86	2.82[a]	3.31	2.98	2.82[a]	3.92	4.02	6.47	5.03
12	3.61	3.87	2.83	3.32	2.99	2.77	3.66	3.83		
(DMSO)	3.34	3.41	2.75	3.12	2.79	2.69	3.67	3.83	6.83	5.36
					2					
2	3.49	3.88	3.03	2.96[a]	2.56	2.96[a]			6.45	4.24,[a] 4.24[a]
7.6	3.51	3.89	3.04	2.97[a]	2.56	2.97[a]				
12	3.51	3.90	3.03	2.97[a]	2.56	2.97[a]				
(DMSO)	3.31	3.48	2.89	2.69	2.40	2.79			6.87	4.92, 4.98

[a] Signals overlap.

the solution was raised to pH 12, but all other signals remained unchanged. This result indicates that deprotonation of a coordinated amine in $Re^{I}(CO)_3$ complexes is not favorable, in contrast to our findings for $Re^{V}O$ analogues of radiopharmaceuticals, where NH deprotonation is common near neutral pH.[26,27,29−31]

We wished to determine whether the solution structure, the X-ray structure, and the computed structure agree. The Karplus type equation[32] ($^3J = 11.0 \cos^2 \Phi - 1.4 \cos \Phi + 1.6 \sin^2 \Phi$) can be used to calculate the coupling constants of **2** in solution by using a torsion angle Φ obtained from the X-ray structure, which allowed us to evaluate the similarities between the solution-state and solid-state structure (and the computed structure for **2**, namely, **7b**). For this purpose, we needed to assign the NMR signals. In the ^{1}H NMR spectrum of **2** in DMSO-d_6, all aliphatic signals were resolved (Table 4). In addition, three broad signals, each integrating for one proton, disappeared when D_2O was added to the NMR sample, and these were assigned to the exchangeable amine protons. The shift of one amine signal (6.87 ppm) was almost identical to that for both **1A** and **1B** (∼6.80 ppm); this signal was assigned to the H1N proton. (All amine signals and protons are designated with an N to differentiate these from CH signals and protons.) Two other signals, at 4.92 and 4.98 ppm, must be from the two H2N protons.

The H3A/H3B and H4A/H4B signals of **2** in DMSO-d_6 were assigned from the correlation spectroscopy (COSY) cross peaks to H1N and H2N signals, respectively. The H1N signal gave only one cross peak with an H3 signal. We assign this to H3B because the H1N−N1−C2−H3B torsion angle in the solid is 44° (the computed torsion angle in **7b** is 42°) and the H1N−N1−C2−H3A torsion angle is −76° (the computed torsion angle in **7b** is −76°). The calculated $^3J_{H1NH3B}$ was larger (5.5 Hz) than $^3J_{H1NH3A}$ (2 Hz). Also, the H1N−H3A COSY cross peak is expected to be too weak, and no H1N−H3A cross peak was found. The calculated coupling constants ^3J agree well with the observed values ($^3J_{H1NH3B} = 4.8$ Hz, $^3J_{H1NH3A} = 1.2$ Hz). One H2N signal had two cross peaks with both H4 signals, and the second H2N signal had only one cross peak (with the upfield H4 signal). The H4 proton with the downfield signal has an ∼90° torsion angle relationship to one of H2N amine protons. In the solid, the H2NA−N2−C4−H4B torsion angle is −81° (the computed torsion angle in **7b** is −93°); thus, we assign the downfield signal (2.79 ppm) to H4B and the upfield signal (2.40 ppm) to H4A. As a result, we assign the H2N signal (4.98 ppm) with two cross peaks to H2NB, and the signal with only one cross peak (4.92 ppm) to H2NA. The H2A/H2B assignments in **2** were based on studies of **1A** and **1B** (next paragraph) and were confirmed by COSY cross peaks to H1N. All assignments (Table 4) were confirmed by nuclear Overhauser enhancement spectroscopy (NOESY) data from the H2A−H3A, H2A−H4A, H2A−H4A, and H2B−H4B cross peaks and by the simulation of the 1D ^{1}H NMR spectrum with ACD/HNMR software.[15]

As mentioned, the H2A/H2B assignments in **1A** and **1B** were made by COSY in DMSO-d_6 from the cross peaks to the H1N signal. The signals from the acetate residue coordinated to the metal, H2A/H2B, have virtually identical coupling patterns for **1A**, **1B**, and **2**. Because the H1N−N1−C2−H2A torsion angle in the solid for **2** is 90° (101° for **1A** and 83° for **1B**; the computed torsion angle in **7b** is 86°), almost no H1N/H2A coupling would be expected ($J = 0$ Hz), and the H2A NMR signal appeared as a doublet (3.31 ppm, $J = 16.8$ Hz). In the solid, the H1N−N1−C2−H2B torsion angle for **2** is ∼ −27° (−16° for **1A** and −35° for **1B**; the computed torsion angle in **7b** is −33°); thus, the H1N/H2B coupling should be weak, and the H2B NMR signal was a doublet of doublets (3.48 ppm, $^3J = 16.8$, 7.2 Hz).

The ^{1}H NMR spectrum of $Re(CO)_3$(ENDACH)-A (**1A**) is very similar to the spectrum of $Re(CO)_3$(ENAC) (**2**). (In Supporting Information, we explain this finding by using Newman projections.) Both **1A** and **1B** differ from **2** by having the additional uncoordinated acetic acid residue (H5A/H5B protons) and two secondary amine groups for which two broad signals were observed at pH 3, each integrating for one proton. The H1N signal was assigned as above. The H2N signal in **1A** was downfield (5.45 ppm) of the H2N signal in **1B** (5.03 ppm), indicating that the shift of the H2N signal in **1A** is diagnostic of the configuration at N2. Although the presence of the carboxyl group complicates the analysis (small shift changes for the H5A/H5B signals at higher pH values), careful ^{1}H NMR studies revealed that the NH centers do not deprotonate at high pH (pH ≈ 12); thus, **1A** and **1B** behave the same as **2**. As for **2**, the assignments of pairs of H2A/H2B, H3A/H3B and H4A/H4B, H5A/H5B spin systems were based on the COSY cross peaks to H1N and H2N signals, respectively, and the assignments were confirmed by NOESY spectra. The 1D ^{1}H NMR spectra of **1A** and **1B** (pH ≈ 3) revealed that the H2A/H2B and H5A/H5B signals have a different AB spin system for the two acetic acid groups. Both H5 protons from the uncoordinated acetic acid group give a sharp doublet of doublets with $^3J = 16.8$, ∼7 Hz. The vicinal coupling constant value of ∼7 Hz corresponds to an av-

(32) Kopple, K. D.; Wiley, G. R.; Tauke, R. *Biopolymers* **1973**, *12*, 627.

eraged coupling consistent with the expected rapid free rotation of the uncoordinated acetic acid group around the N2−C5 bond. These results, consistent with a strong H2N/H5 coupling, are supported by X-ray data for the solids (H2N−N2−C5−H5A torsion angles of −178° for **1A** and **1B**, and H2N−N2−C5−H5B torsion angles of 65° and 62° for **1A** and **1B**, respectively) and by density functional calculations (computed H2N−N2−C5−H5A torsion angles of −151° and −157° for **9b** and **9c**, respectively, and H2N−N2−C5−H5B torsion angles of 90° and 84° for **9b** and **9c**, respectively). From the Karplus relationship, the relevant coupling constants were calculated using a torsion angle Φ obtained from the X-ray structure. In gauche coupling with $\Phi \approx 60°$, the value for $^3J_g \approx 2.5$ Hz, and in trans coupling with $\Phi \approx 180°$, the value for $^3J_t \approx 12$ Hz. If two rotamers are roughly equally abundant and at equilibrium, fast rotation results in a vicinal coupling constant which is the arithmetic average, $^3J \approx 7$ Hz. This coupling value is consistent with the experimental result.

To assess the $Re(CO)_3$(ENDACH) equilibrium position, each pure complex, **1A** and **1B**, was dissolved in D_2O in an NMR tube and the pH was adjusted to pH 11. During the first day, spectra were recorded every 3 h and then once a day for 7 days. A sample from each measurement was analyzed by HPLC. After the third day, no spectral changes were observed and the spectra for both solutions were identical, showing a 70:30 mixture of isomers **1A** and **1B**, respectively. The same ratio was obtained by HPLC analysis.

Density Functional Calculations. Geometry. In designing radiopharmaceuticals, it is useful to have methods for performing computer modeling. Because we have extensive structural data and solution data, optimization of methods for Tc/Re complexes through density functional theory on the Tc/$Re(CO)_3$(ENDACH) type species (and other [Re/$Tc(CO)_3$L] molecules) (**3**−**9**, Figures 4 and 5) appeared to be warranted.

The comparative analysis for corresponding Tc and Re species shows slightly shorter Re-donor bond distances. Differences for the bond angles are also small (within 2°). Carbonyl C−O bond distances are shorter in Tc complexes than in Re complexes. These data suggest a lower π-back-donation for Tc than for Re. The computed structures from this work compare well with X-ray data for *fac*-[$Re(CO)_3$-(H_2O)(phenanthroline)]$^+$ [33] and for *fac*-[$Re(CO)_3$(OH)(4,4′-dimethyl-2,2′-bipyridine)],[34] and with experimental data from this work.

The simple [$Re(CO)_3(NH_3)_2(H_2O)$]$^+$ model (**3**) reproduces well (within 0.05 Å) the Re−C and Re−N bond distances found in the solid state for **1A**, **1B**, and **2**, whereas the computed Re−OH_2 distance is significantly longer (by 0.14 Å) than the experimental Re−O distance for the coordinated carboxyl group. This finding is reasonable on the basis of the strong ionic contribution affecting the latter Re−O bond. The computed bond angles for **3** are in good agreement with

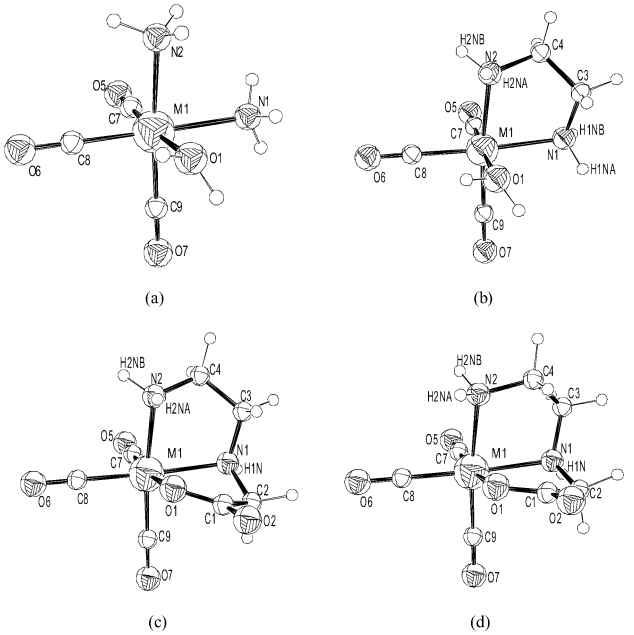

Figure 4. ORTEP-style drawings of the computed molecules (a) [$M(CO)_3(NH_3)_2(H_2O)$]$^+$, **3**; (b) [$M(CO)_3$(EN)(H_2O)]$^+$, **5**; (c) $M(CO)_3$(ENAC), **7a**, δ-EN; and (d) $M(CO)_3$(ENAC), **7b**, λ-EN. In the cases shown M = Re, however the models for M = Tc (**4**, **6**, **8a**, and **8b**, respectively) are essentially superimposable. For the sake of clarity, the atom labeling for the hydrogen atoms is not depicted.

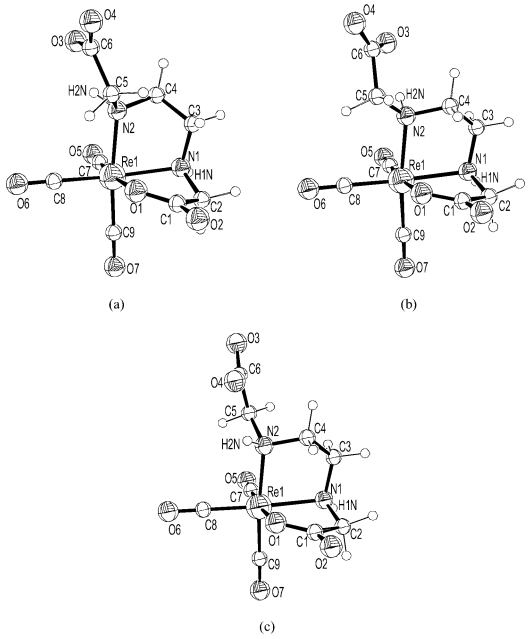

Figure 5. ORTEP-style drawings of the computed [$Re(CO)_3$(ENDAC)]$^-$ species: isomer A δ-EN −*anticlinal*-CH_2COO^- **9a** (a); isomer A λ-EN −*antiperiplanar*-CH_2COO^- **9b** (b); and isomer B λ-EN +*antiperiplanar*-CH_2COO^- **9c** (c). For the sake of clarity, the atom labeling for the hydrogen atoms is not depicted.

experiment, except for N1−Re−O1 and N1−Re−N2, which are smaller by ∼7° with respect to the experimental values, mostly because of the restraints due to five-membered chelate rings in **1A**, **1B**, and **2**. The results for **3** were similar to those for the Tc analogue, **4**.

In the aqua-models, replacement of the two NH_3 molecules by EN improved the N1−M−N2 angle in the refined structure, even though the N1−M−O1 angle is still

(33) Connick, W. B.; Di Bilio, A. J.; Schaeffer, W. P.; Gray, H. B. *Acta Crystallogr.* **1999**, *C55*, 913.
(34) Gibson, D. H.; Yin, X.; He, H.; Mashuta, M. S. *Organometallics* **2003**, *22*, 337.

large. Furthermore, the *cis*-O−M−N bond angles (computed and experimental) are all smaller than 90°, whereas the *cis*-O−M−C angles are all greater than 90°, no matter whether chelation is operative and the oxygen donor is from neutral H_2O or from anionic CO_2^-. The C−M−C bond angles have idealized values of 90° (within 1°, computed; within 3°, experimental). This analysis reveals that $[M(CO)_3(NH_3)_2(H_2O)]^+$ is a good model to simulate quickly the main features of the $M(CO)_3(sp^3N)_2(sp^3O)$ coordination spheres to an acceptable degree of accuracy.

The metal−donor bond distances computed for **9b** ($[Re(CO)_3(ENDAC)]^-$, isomer A λ-EN −*antiperiplanar*-CH_2COO^-) and the corresponding distances found for **1A** (also λ-EN) differ by less than 0.01 Å, except for Re−N1 (0.045 Å) and Re−N2 (0.018 Å). (In the crystal, H1N of **1A** is involved in a hydrogen bond to cocrystallized water (N···O, 2.959 Å; N−H···O, 156°), and H2N is a hydrogen donor to a carboxyl group (intermolecular; N···O, 2.995 and 3.091 Å; N−H···O, 153 and 151°). These effects are not present in the computation (isolated molecule, **9b**).) The agreement for the metal donor bond lengths for **9c** and **1B** is even better. This relationship is confirmed by the analysis of the computed **7b** structure with the experimental **2**·H_2O structure. The Re−N1 bond length is 0.036 Å longer for **7b** than that for **2**. Again, strong N1−H···O hydrogen bonding to cocrystallized water occurs (N···O, 2.863 Å; N−H···O, 156°). Furthermore, the N1−H atom for **1B** is involved in a weaker intermolecular hydrogen bond (in this case to C2═O2 carbonyl of the metal-bound carboxylate) than the corresponding hydrogen bonds for **1A** and **2** (involving cocrystallized water molecules). For **1B**, the experimental structural parameters for N1−H···O2 ($-x + 1$, $y + {}^1/_2$, $-z + {}^1/_2$) are N···O, 3.018 Å; N−H···O, 139°.

Computed C−O bond distances (1.188−1.197 Å for **9a**−**c**,Table 2) compare well with the experimental values for **1A** and **1B** (1.150−1.163 Å) and computed values (1.161−1.199 Å) for a series of neutral and anionic Mn−CO complexes, as optimized through density functional theory (DFT) methods.[35] The N−C and C−C bond distances for the ethylene bridge are reproduced well by computations, the largest difference from experimental values being 0.026 Å. Computed bond angles (Table 3) at the metal center compare well with the experimental values, the largest difference being 3.6° for C7−Re1−C8 (**9b** and **1A**). The computed conformation of the chelate ring for **9b** is λ, as found for **1A**, and the bond distances and angles within the ENDAC ligands are reproduced well by the calculation (Table 3). On changing the conformation of the EN bridge from λ to δ in the starting model structure, another relative minimum energy structure went to convergence (**9a**). Some different orientations of the dangling acetate chain occur in the computed structures (**9b**,**c**) when compared to the observed ones (**1A**, **1B**). Note that the input structures for the optimization procedure for **9b** and **9c** are based on the X-ray structures, **1A** and **1B**, respectively. The computed torsion angles, Re1−N2−C5−C6 and N2−C5−C6−O, are −151.1° and 14.6° for **9b** and 157.2° and −18.5° for **9c**, whereas the corresponding experimental values are −167.4° and 4.5° (**1A**) and 65.5° and 29.7° (**1B**), respectively. It is reasonable to assume that intermolecular forces in the solid state and even in solution, especially the hydrogen bonds, can influence significantly the orientation of the acetate groups, at least within certain regions of the conformational space. These results indicating several possible orientations are consistent with the NMR results that suggest dynamic motion of the dangling acetate. The comparative analysis between **7a,b** and **9a**−**c** (Tables 2 and 3) shows that the coordination sphere structure does not change appreciably when the dangling CH_2COO^- group is present. As a consequence, this dangling group probably influences the intermolecular interactions and the solubility but not the electronic properties of the complex.

Table 5. Total Electronic Energy (Hartrees[a]) for the Optimized Structures

molecule	*E*
3, $[Re(CO)_3(NH_3)_2(H_2O)]^+$	−608.513467
4, $[Tc(CO)_3(NH_3)_2(H_2O)]^+$	−609.475498
5, $[Re(CO)_3(EN)(H_2O)]^+$	−685.908949
6, $[Tc(CO)_3(EN)(H_2O)]^+$	−686.870195
7a, $Re(CO)_3$(ENAC), δ-EN	−836.950698
7b, $Re(CO)_3$(ENAC), λ-EN	−836.951867
8a, $Tc(CO)_3$(ENAC), δ-EN	−837.905395
8b, $Tc(CO)_3$(ENAC), λ-EN	−837.906451
9a, $[Re(CO)_3(ENDAC)]^-$, isomer A δ-EN −*anticlinal* -CH_2COO^-	−1064.272834
9b, $[Re(CO)_3(ENDAC)]^-$, isomer A λ-EN −*antiperiplanar*-CH_2COO^-	−1064.275836
9c, $[Re(CO)_3(ENDAC)]^-$, isomer B λ-EN +*antiperiplanar*-CH_2COO^-	−1064.274537

[a] 1 hartree = 627.51 kcal.

Energy. From the total electronic energy computed for the optimized molecules (Table 5), it is evident that the orientation of the N−C−C−N moiety plays a significant role in determining which $[Re(CO)_3(ENDAC)]^-$ species is the most stable. The most stable species is the A, λ-EN conformer (**9b**), in agreement with the experimental results. Furthermore, the energy gap between **9b** and **9c** (0.815 kcal mol^{-1}) corresponds at 298 K to an 80:20 molar ratio, which compares well with the 70:30 ratio found experimentally. Thus, intermolecular interactions and entropic effects are similar for the isomers of $[Re(CO)_3(ENDAC)]^-$. A similar trend does exist for **7a** and **7b**, which differ by 0.734 kcal mol^{-1}. The A, δ-EN conformer (**9a**) is 1.883 kcal mol^{-1} less stable than the A, λ-EN conformer (**9b**); consequently, the amount of A, δ-EN conformer in solution is negligible when compared to the A, λ-EN conformer at room temperature. The destabilizing factor is the contact distance between the O1 donor and C5 from the free acetate chain, which is shorter (3.08 Å) in the A, δ-EN conformer (**9a**) than that in the A, λ-EN conformer (**9b**) (3.40 Å). Consistent with this interpretation, the O1−Re1−N2 bond angle is larger by 3.3° for **9a** compared to that of **9b**.

Conclusions. We have studied the coordination capabilities of ligands ($ENDACH_2$ and ENACH) with aliphatic amines as the only nitrogen donors toward the *fac*-$\{M(CO)_3\}^+$ core. Tridentate ligation is observed when

(35) Andrews, L.; Zhou, M.; Wang, X.; Bauschlicher, C. W. *J. Phys. Chem. A* **2000**, *104*, 8887.

two sp^3 nitrogen donors and at least one sp^3 carboxyl oxygen donor are available. The ligands formed well-defined complexes with the $M(CO)_3$ fragment. The presence of a secondary amine in protonated form is the source of isomer formation. The NH center (N2) bearing the dangling $CH_2CO_2^-$ group has a different configuration for the two isomers. All analytical and spectroscopic data as well as density functional calculations indicate that the endo configuration of the N2 amine is favored. Because the coordinated NH group is very weakly acidic, high pH values are needed to catalyze isomerization at a rate relevant to the decay half time (~6 h) for ^{99m}Tc imaging agents.

Finally, the computational studies in this work show that density functional methods employing even small basis sets (LANL2DZ all atoms) model the $[Re(CO)_3(ENDAC)]^-$ and $Re(CO)_3(ENAC)$ complexes very well and that the trend of computed electronic energies predict well the populations of isomers and conformers for $M(CO)_3(sp^3N)_2(sp^3O)$ complexes with tridentately chelated $ENDAC^{2-}$ and $ENAC^-$ ligands. Indeed, preliminary computations performed on the same complexes by using more expanded and diffuse basis sets (e.g., 6-31+G** for C, H, N, O atoms) improve the quality of C−O (carbonyl ligand) bond lengths but do not significantly change either the result for all other geometrical parameters or the trend of total electronic energy values for conformers or isomers.

Acknowledgment. This work was supported by the National Institutes of Health (Grant No. DK38842). We thank Dr. Kenneth Hardcastle of Emory University for useful discussions and for determining the structures of **1A**, **1B**, and **2**, by using instruments supported by NIH Grant No. S10-RR13673 and NSF Grant No. CHE 9974864. The authors thank CINECA (Inter-University Computing Center, Casalecchio di Reno, Bologna, Italy) for the use of the Origin 3800 SG machine and the University of Siena for funding. We thank Dr. Patricia A. Marzilli for her invaluable comments during the preparation of the paper.

Note Added after ASAP: Isomer A was incorrectly published as **1A** in the caption to Figure 5 in the version posted ASAP October 23, 2004; the corrected version was posted October 28, 2004.

Supporting Information Available: Additional explanations of NMR shifts employing Newman projections. Tables of atomic coordinates for structures computed via DFT methods. X-ray crystallographic data for **1A**, **1B**, and **2** in CIF format. This material is available free of charge via the Internet at http://pubs.acs.org.

IC049544I